

# Incorporating travel behavior regularity into passenger flow forecasting

Zhanhong Cheng<sup>a,b</sup>, Martin Trépanier<sup>b,c</sup>, Lijun Sun<sup>a,b,\*</sup>

<sup>a</sup>Department of Civil Engineering, McGill University, Montreal, QC H3A 0C3, Canada

<sup>b</sup>Interuniversity Research Centre on Enterprise Networks, Logistics and Transportation (CIRRELT)

<sup>c</sup>Department of Mathematics and Industrial Engineering, Polytechnique Montreal, Montreal, QC H3T 1J4, Canada

## Abstract

Accurate forecasting of passenger flow (i.e., ridership) is critical to the operation of urban metro systems. Previous studies mainly model passenger flow as time series by aggregating individual trips and then perform forecasting based on the values in the past several steps. However, this approach essentially overlooks the fact that passenger flow consists of trips from each individual traveler with strong regularity rooted in their travel behavior. For example, a traveler's work trip in the morning can help predict his/her home trip in the evening, while this fact cannot be explicitly encoded in standard time series models. In this paper, we propose a new passenger flow forecasting framework by incorporating the generative mechanism into standard time series models. In doing so, we focus on forecasting boarding demand, and we introduce returning flow from previous alighting trips as a new covariate, which captures the causal structure and long-range dependencies in passenger flow data based on travel behavior. We develop the return probability parallelogram (RPP) to summarize the causal relationships and estimate the return flow. The proposed framework is evaluated using real-world passenger flow data, and the results confirm that the returning flow—a single covariate—can substantially and consistently benefit various forecasting tasks, including one-step ahead forecasting, multi-step ahead forecasting, and forecasting under special events. This study can be extended to other modes of transport, and it also sheds new light on general demand time series forecasting problems, in which causal structure and the long-range dependencies are generated by the behavior patterns of users.

**Keywords:** Ridership forecasting, public transport systems, time series, travel behavior regularity

## 1. Introduction

Recent years have witnessed the rapid development of metro systems and the continued growth of metro ridership worldwide (Union Internationale des Transports Publics (UITP), 2018). As an efficient and high-capacity transportation mode, the metro is also playing an ever-important role in shaping future sustainable transportation. Given the growing importance of metro systems, it is critical to have a good understanding of passenger demand patterns to support service operation. A particularly important task is to make accurate and real-time forecasting of passenger demand/ridership, which plays a vital role in a wide range of applications, including service scheduling, crowd management, and disruption response, to name but a few.

Short-term passenger flow forecasting has always been an important topic in public transport research. Most existing studies consider passenger flow data as time series and follow similar methods as those applied in traffic flow forecasting. For example, statistical time series models have been widely applied to ridership forecasting problems, including auto-regressive integrated moving average (ARIMA) (Williams and Hoel, 2003; Ding et al., 2017; Chen et al., 2020a), exponential smoothing (Tan et al., 2009), and state-space/Kalman filter (Stathopoulos and Karlaftis, 2003; Jiao et al., 2016). Essentially, these classical time series models are linear in nature; to better characterize the non-linearity in time series data, recent research starts regarding the forecasting a supervised machine learning problem. On this track, some representative supervised learning models have been applied, such as support vector machine (SVM) (Chen et al., 2011; Sun et al., 2015), artificial neural network (ANN) (Vlahogianni et al., 2005; Tsai et al., 2009; Li et al., 2017), random forest (Toqué et al., 2017), and recurrent neural network (RNN)/long short-term memory (LSTM) as emerging deep learning approaches (Hao et al., 2019; Liu et al., 2019). The aforementioned research mainly focuses on modeling a univariate time series for a single metro station. However, the metro system is a network in

\*Corresponding author. Address: 817 Sherbrooke Street West, Macdonald Engineering Building, Montreal, Quebec H3A 0C3, Canada

Email addresses: zhanhong.cheng@mail.mcgill.ca (Zhanhong Cheng), mtrepanier@polymtl.ca (Martin Trépanier), lijun.sun@mcgill.ca (Lijun Sun)

which stations exhibit strong spatial and temporal correlations/dependencies. To extend the univariate analysis to network-wide passenger flow forecasting, some state-of-the-art models have been proposed to better characterize the complex spatiotemporal patterns and dynamics. For example, [Gong et al. \(2018\)](#) proposed matrix factorization models to estimate passenger flow data for each origin-destination (OD) pair; [Chen et al. \(2020b\)](#) developed graph convolutional network (GCN) models to capture the complex spatiotemporal dependencies in a metro network. These new machine learning-based models have shown superior performance over traditional time series models, and they are more effective in capturing the complex patterns by incorporating domain knowledge and external features such as weather, event, time of day, and day of week.

In all the studies mentioned above, passenger flow data is generally modeled as an aggregated count time series, obtained by counting the number of unique card ID in smart card transactions. Although these models are effective, we would argue that the most important characteristic of passenger flow is overlooked due to the aggregation: passenger flow consists of the movement of individuals with strong regularity rooted in their travel behavior. For instance, if a passenger alights at a metro station for work in the morning, he/she will probably depart at the same station when he/she goes home in the evening. If he/she does not travel in the morning, it becomes less likely we will observe a corresponding return trip. This example clearly shows that past trips should be utilized to predict future demand, and individual travel behavior actually can result in causal structure and long-range dependencies in passenger flow time series data. Some recent studies have shown that the behavioral component plays a substantial role in passenger flow forecasting tasks, in particular when passengers' travel patterns in metro systems are highly regular ([Sun et al., 2013](#); [Goulet-Langlois et al., 2017](#); [Zhao et al., 2018](#)). Therefore, when developing a passenger flow forecasting model, it is essential to integrate this type of behavior-driven and long-range dependency in addition to the local input (e.g., the past  $n$  steps in the time series).

The goal of this study is to explore the potential of incorporating an additional travel behavior component into the forecasting of passenger flow time series. Specifically, we propose a new scheme to forecast boarding/incoming passenger demand at a station by integrating historical alighting time series at the same station. We define returning passengers as those who finish their first trip at station  $s$  and also start their second trip at the same station. In other words, returning passengers refer to the individuals who stay at station  $s$  to perform an activity (e.g., home and work). In general, these return trips are not random and often exhibit strong regularity due to the activities performed. This motivates us to forecast the incoming/boarding demand from these "returning passengers" using the information of their previous trips. To achieve this, we introduce a new concept of return probability parallelogram (RPP) to better estimate returning flow, and we find that the estimated returning flow highly correlates with the overall boarding demand in a real-world data set. To further quantify the benefits of incorporating this returning flow measure, we evaluate the proposed models for short-term forecasting, long-term forecasting, and forecasting under special events. Our results show that incorporating returning flow as an additional variable will consistently improve the accuracy of forecasting.

The idea of leveraging trip-level information has been introduced and examined in some recent studies, which predict the alighting flow of a station using the recent boarding flow from other related stations (see e.g., [Li et al., 2017](#); [Hao et al., 2019](#); [Liu et al., 2019](#)). However, the large number of boarding-alighting station pairs makes it difficult to learn an informative model at a trip level, and eventually these studies develop deep neural networks to learn the correlation from the aggregated count data in a purely data-driven approach. Our model, instead, uses the alighting of "this trip" to predict the boarding of the "next trip", where the alighting and the boarding stations are usually the same ([Barry et al., 2002](#); [Trépanier et al., 2007](#)). We examine this idea on a boarding flow forecasting application, which is more important to service operation and planning. The "returning flow" proposed in this paper is solely based on the intrinsic travel regularity of travelers and it does not require external information/knowledge. Our work is closely related to [Zhao et al. \(2018\)](#), which proposes a probabilistic model to predict the next trip for an individual based on his/her trip history. However, instead of predicting individual trips, our primary goal is to forecast the overall passenger flow to support the decision making in service operation. In doing so, we estimate the returning flow in an aggregated approach; therefore, the framework does not require individual-based data sets that are confidential and sensitive for privacy reasons. The main contribution of this work is summarized as follows.

- We define returning flow to characterize the causal structure and long-range dependencies in passenger flow data, which are essentially overlooked in previous time series-based studies.
- We integrate returning flow as an additional covariate into standard time series models, and the proposed behavior-integrated model shows consistently improved performance in our case studies based on a real-world data set.
- Our model also provides a new approach to forecast passenger flows and detect anomalies under special events.

To the best of our knowledge, this is the first research that incorporates a travel behavior component into the longstanding passenger flow forecasting problem. The remainder of the paper is organized as follows. Section 2 introduces the concept of returning flow and return probability parallelogram as the tool to integrate travel behavior regularity into the passenger flow forecasting framework. In section 3, we develop case studies based on real-world smart card data and we demonstrate the effectiveness our models under different scenarios. Finally, we summarize the conclusion and future research in section 4.

## 2. Methodology

In this section, we introduce returning flow and the return probability parallelogram as two fundamental variables in developing the behavior-based boarding flow forecasting framework. The proposed forecasting models are constructed by integrating returning flow as a new feature/covariate into traditional time series forecasting models. Before introducing the behavior variables, we first give a brief description of the passenger flow forecasting problem.

### 2.1. Problem description

Suppose that in a metro system we have access to all smart card transactions, i.e., we know the anonymous ID of passengers, the time and the location of both boarding (tapping-in) and alighting (tapping-out) for each trip. In this case, a station  $s$  will generate two passenger flow time series: the alighting/arriving flow for passengers with station  $s$  as their destination, and the boarding/incoming flow for passengers who start their trips from station  $s$ . We denote by  $y_t^s$  and  $m_t^s$  the boarding flow and the alighting flow at station  $s$  in time interval  $t$ , respectively.

We focus on the case of forecasting the boarding flow  $y_t^s$ . Given some recent observations  $y_1^s, \dots, y_{t-1}^s, y_t^s$ , our goal is to predict the values of  $y_{t+1}^s, y_{t+2}^s, \dots, y_{t+L}^s$  in the next  $L$  time steps/intervals. This is a standard time series analysis problem, and it is straightforward to apply traditional statistical models such as ARIMA to perform forecasting. However, in this paper, we want to examine if we can achieve better forecasting results by utilizing the additional information from alighting flow  $m_t^s$  and the behavioral regularity of passengers.

### 2.2. Returning flow

We begin our model by introducing the concept of the “returning flow”. To facilitate model development, we divide all the passengers associated with stations  $s$  (both boarding and alighting) into two groups (see Figure 1):

(G1) Passengers who alight at station  $s$ ;

(G2) Passengers who board at station  $s$  without a previous trip alighting at  $s$ .

Group		$t-h$	$\dots$	$t-2$	$t-1$	$t$	$t+1$	$t+2$	$\dots$	$t+L$
G1	A	○ $\longrightarrow$ ●								
		○ $\longrightarrow$ ●					○ $\cdots \longrightarrow$ ●			
							○ $\cdots \longrightarrow$ ●			
							○ $\cdots \longrightarrow$ ●			
G2	B			○		○				
						●				
	sum ○ in G1	$m_{t-h}^s$	$\dots$	$m_{t-2}^s$	$m_{t-1}^s$	$m_t^s$				
	sum ● in G1+G2	$y_{t-h}^s$	$\dots$	$y_{t-2}^s$	$y_{t-1}^s$	$y_t^s$	$\hat{y}_{t+1}^s$			

○ represents alighting, ● represents boarding,  
 $\longrightarrow$  represents observed trip chain,  $\cdots \longrightarrow$  represents trip chain to be predicted.

Figure 1: Illustration of two passenger groups (G1/2) and the boarding demand forecasting problem at station  $s$ .

With this definition, we can model the boarding flow  $y_t^s$  by combining the boarding activities in the two groups. The passengers in G1 can be further separated into two subgroups given if they have their next trip originating from station  $s$  within a certain time window. We define the subgroup with a following trip as G1A and the other as G1B. Thus, G1A actually consists of those passengers who conduct certain activities (e.g., home/work) at station  $s$ . We

define “returning flow” at time  $t$  as the number of people in G1 who will finish their activities and start their return trips at time  $t$ , denoted by  $r_t^s$ . In fact, these chained trips (with departing station identical to the alighting station of a previous trip) make up a substantial component of all trips. For the Guangzhou metro in our case study, we actually find that chained trips cover about 60% of all trips. Therefore, our hypothesis is that having the “returning flow” as an additional variable will enhance the forecasting of  $y_{t+1}^s$ . We refer to this new model with  $r_{t+1}^s$  as a covariate as M1:

$$\text{M1: } y_{t+1}^s = f(y_{1:t}^s, r_{t+1}^s). \quad (1)$$

We consider a standard time series model without any additional variables as a baseline (M0):

$$\text{M0: } y_{t+1}^s = f(y_{1:t}^s). \quad (2)$$

The concept of “returning flow” is very simple and we would expect  $r_{t+1}^s$  contributes significantly given that the boarding demand is largely composed of the returning flow. However, it should be noted that we do not have access to  $r_{t+1}^s$ , as the returning flow in G1 is only observed until time  $t$  (i.e., those dashed arrows in Figure 1). Therefore, in practice, we need to first estimate  $\hat{r}_{t+1}^s$  and then use it as a proxy in M1. A possible alternative is to use  $r_t^s$ —which we have access in real-time—instead of  $\hat{r}_{t+1}^s$  as the covariate. We define this alternative model as M2 and also use it as a baseline model:

$$\text{M2: } y_{t+1}^s = f(y_{1:t}^s, r_t^s). \quad (3)$$

### 2.3. Return probability parallelogram (RPP)

In this subsection, we propose a simple method to estimate  $\hat{r}_{t+1}^s$  in M1 based on the time series of alighting flow  $m_t^s$ . Our fundamental assumption is that there exists a universal distribution  $p^s(\tau_{\text{boarding}} | \tau_{\text{alighting}})$  characterizing the conditional probability that a passenger in G1 who alights at time  $\tau_{\text{alighting}}$  will start his/her returning trip at time  $\tau_{\text{boarding}}$ . Note that we define  $p^s$  on the whole group G1, so the subgroup G1B is also modeled in this distribution. Assuming the length of returning time window is  $H$  when we define G1A, for the passengers who alight at time  $t_a$  we have:

$$\sum_{t=t_a+1}^{t_a+H} p^s(\tau_{\text{boarding}} = t | \tau_{\text{alighting}} = t_a) + p^s(\tau_{\text{boarding}} = \text{NA} | \tau_{\text{alighting}} = t_a) = 1, \quad (4)$$

in which the term  $p^s(\tau_{\text{boarding}} = \text{NA} | \tau_{\text{alighting}} = t_a)$  represents the conditional probability of an arriving passenger does not return (i.e., subgroup G1B).

If the conditional distribution  $p^s(\tau_{\text{boarding}} | \tau_{\text{alighting}})$  is available for all  $\tau_{\text{alighting}}$ , we can estimate the expectation of the returning flow  $r_{t+1}^s$  at time  $t+1$  by:

$$\hat{r}_{t+1}^s = \sum_{h=1}^H m_{t-h+1}^s p^s(\tau_{\text{boarding}} = t+1 | \tau_{\text{alighting}} = t-h+1). \quad (5)$$

It is important to note that the estimation of  $\hat{r}_{t+1}^s$  using Eq. (5) is very different from predicting  $\hat{r}_{t+1}^s$  using a time series model based on past observations. This is because a simple time series model such as ARIMA cannot characterize the unique generative mechanisms (e.g., come-and-return) and the corresponding long-range dependencies/causal structure provided by these mechanisms in the passenger flow data.

The time window length  $H$  is an additional parameter to be determined before applying Eq. (5). To choose an appropriate  $H$ , we quantify the inter-trip time/duration ( $\tau_{\text{boarding}} - \tau_{\text{alighting}}$ ) for all those passengers with both the alighting trip and the next boarding trip at the same station. We conduct this analysis on the Guangzhou metro data set. Figure 2 shows the distribution of the inter-trip time of two representative stations in a commercial area and a residential area, respectively. The distribution is obtained by aggregating all alighting records on a typical Monday, and we track the returning flow within 48 hours after the alighting. The return time intervals in both stations are characterized by a bi-modal pattern. The first peak (less than 3 hours) corresponds to certain short-duration activities. The longer peaks largely correspond to “work” activities (9-12 hours) in the commercial area and “home” activities (10-16 hours) in the residential area, respectively. More importantly, as we can see, almost all of the return trips start within a 24-hour window after finishing previous trips. Therefore, for simplicity, we only take the alighting flow within the past 24 hours into account when estimating  $\hat{r}_{t+1}^s$ .

After determining  $H$ , our next task to obtain a good estimate of the conditional probability distribution  $p^s(\tau_{\text{boarding}} | \tau_{\text{alighting}})$ . However, the current formulation involves a set of conditional probabilities for each value of

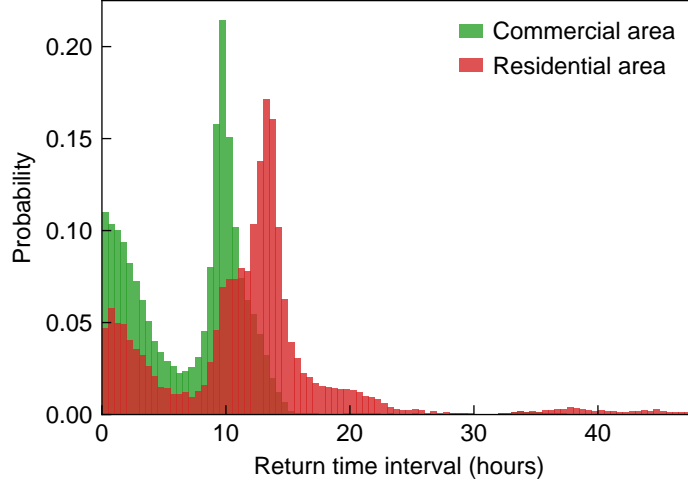


Figure 2: The density histogram of the return time interval ( $\tau_{\text{boarding}} - \tau_{\text{alighting}}$ ) of two example stations.

$\tau_{\text{alighting}}$ , making it difficult to estimate. For simplicity, we assume that the conditional distributions are universal across different days:

$$\begin{aligned} p^s(\tau_{\text{boarding}} = t_b \mid \tau_{\text{alighting}} = t_a) &= p_0^s(\text{future window}(t_b) \mid \text{window of day}(t_a)) \\ &= p_0^s(\text{window of day}(t_a) + t_b - t_a \mid \text{window of day}(t_a)), \end{aligned} \quad (6)$$

where we refer to the reduce distribution  $p_0^s$  as return probability parallelogram (RPP).

As the new conditional distribution  $p_0^s$  is defined given the time of day of  $t_a$ , we can estimate it using historical trip data of passengers in group G1A (i.e., the solid arrows in Figure 1). We use Figure 3 to illustrate the idea of RPP. Panel (a) and (b) show two sets of conditional distributions for a commercial area and a residential area, respectively, in Guangzhou metro. The resolution for time slot is set to half an hour, and the range is from 6:00 to 24:00 (operation time of the metro system). Note that in this parallelogram representation we concatenate the 24:00 of day  $k$  and the 6:00 of day  $k+1$  on the horizontal axis. There are two blank triangles in this diagram: the one on the left corresponds to the  $t_b \leq t_a$ , where the distribution is not defined; the one on the right corresponds to the conditional probability with  $t_b > t_a + H$  ( $H = 48$  for 24 hours), which is also ignored for simplicity. It should be noted that in RPP the sum of each row is less than 1, as it does not include the passengers in G1B (with no returning trips, i.e.,  $\tau_{\text{boarding}} = \text{NA}$ ). With this formulation, we can replace  $p^s(\tau_{\text{boarding}} = t+1 \mid \tau_{\text{alighting}} = t-h+1)$  in Eq. (5) by the corresponding conditional probability in RPP.

As shown in Figure 3, it is obvious that different stations exhibit different RPP patterns. For example, for the commercial station in Figure 3(a), most trips arrive (alight) in the morning and return in the evening on the same day, which essentially captures work activities. It is very rare to see returning trips on the next day. For the station in residential area in Figure 3(b), on the contrary, we can see that the distribution mainly characterizes home activities, where alighting flow generally peaks in the evening and the returning flow concentrates in the morning of the next day. The RPP representation demonstrated in Figure 3 further suggests that the unique come-and-return dynamics for a station should be considered in passenger flow forecasting applications.

### 3. Experiments

In this section, we conduct numerical experiments to evaluate the effectiveness of behavior-integrated models. We choose the standard SARIMA model as the core model for time series forecasting (M0). On top of this model, we create two SARIMA-X models—M1 and M2—by simply incorporating the estimated  $\hat{r}_{t+1}^s$  and the observed  $r_t^s$  as an additional covariates, respectively. We evaluate the performance of these models in three scenarios: 1) one-step ahead forecasting, 2) multi-step ahead forecasting, and 3) forecasting under special events. We use half an hour as the temporal resolution in all experiments.

#### 3.1. ARIMA model

We choose seasonal ARIMA as the main baseline model—M0. ARIMA is a well-established time series forecasting model and it has been widely used in traffic/passenger flow forecasting (Williams and Hoel, 2003; Ding et al., 2017;

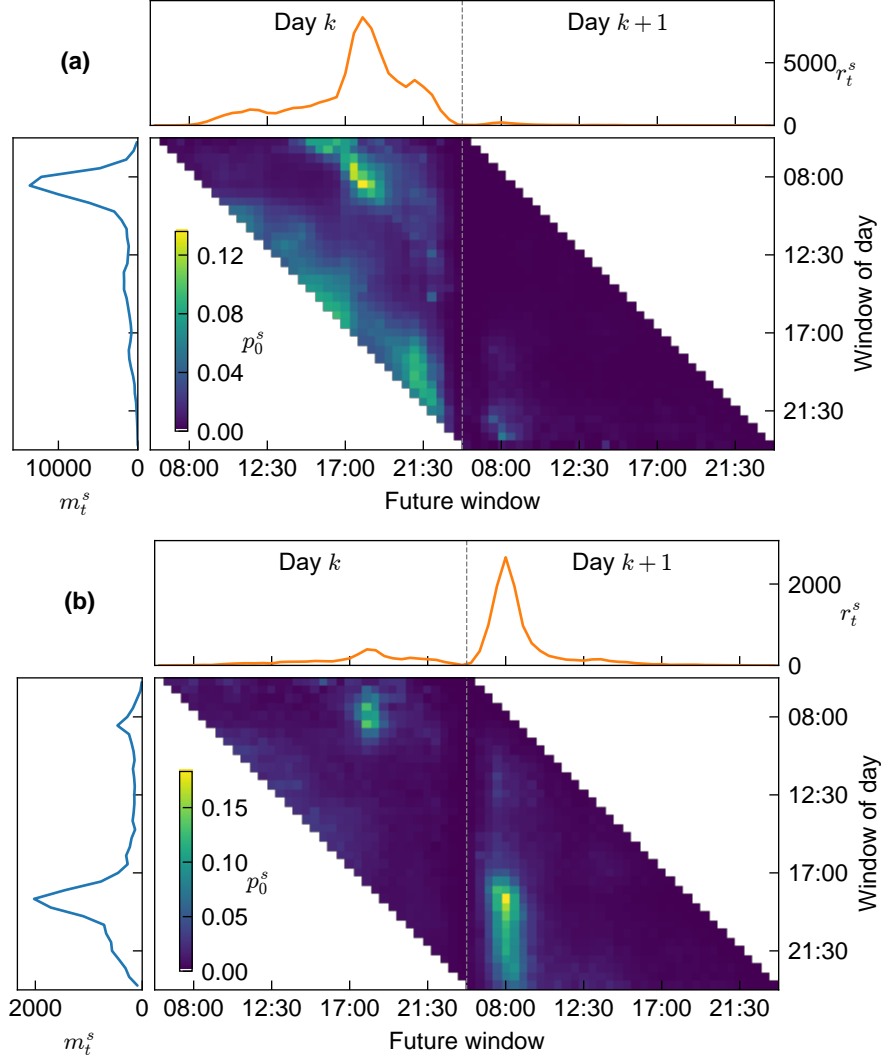


Figure 3: The return probability parallelogram (RPP), the alighting flow  $m_t^s$ , and the returning flow  $r_t^s$  for two representative stations: (a) A typical station in commercial areas. (b) A typical station in residential areas.

Chen et al., 2020a). Considering the strong periodicity from day to day, we apply Seasonal ARIMA (SARIMA) to model passenger flow. Here we give a brief introduction of the SARIMA model, and we refer readers to Hyndman and Athanasopoulos (2018) for a comprehensive review about time series models. A SARIMA model is usually denoted by  $ARIMA(p, d, q)(P, D, Q)[m]$ , where  $p$ ,  $d$ , and  $q$  represent the order of autoregressive, differencing, and moving-average;  $P$ ,  $D$ , and  $Q$  are the order of autoregressive, differencing, and moving-average for the seasonal part; and  $m$  is the number of period in each season. For a time series  $y_1, \dots, y_t$  with covariate  $x_1, \dots, x_t$ . The  $ARIMA(p, d, q)(P, D, Q)[m]$  model takes the following form

$$\Phi(B)(1 - B^m)^D \phi(B)(1 - B)^d (y_t - a - bx_t) = \theta(B)\Theta(B)e_t, \quad (7)$$

where  $B$  is the backshift notation defined by  $B^a y_t = y_{t-a}$ ,  $\Phi(B) = (1 - \Phi_1 B^m - \dots - \Phi_P B^{P*m})$ ,  $\phi(B) = (1 - \phi_1 B - \dots - \phi_p B^p)$ ,  $\theta(B) = (1 + \theta_1 B + \dots + \theta_q B^q)$ , and  $\Theta(B) = (1 + \Theta_1 B + \dots + \Theta_Q B^Q)$ ;  $\Phi_i$ ,  $\Theta_i$ ,  $\phi_i$ ,  $\theta_i$ ,  $a$ , and  $b$  are parameters to be estimated, and  $e_t$  is an error assumed to follow a white noise process (i.e., zero mean and iid).

When using external covariate(s), Eq. (7) is equivalent to a regression model with ARIMA errors; the part not explained by the covariate(s) is modeled by an ARIMA model.



### 3.2. Model selection and evaluation

We apply the same order of SARIMA to the demand time series for all the stations. The seasonal frequency is set to  $m = 36$  (i.e., daily, from 6:00 to 24:00, as we use half an hour as the temporal resolution). For most stations, after a seasonal differencing, the Augmented Dickey-Fuller (ADF) test (Dickey and Fuller, 1979) indicates no further differencing is required to make the time series stationary, we thus set  $D = 1$  and  $d = 0$ . We search over possible models and finally select ARIMA(2, 0, 1)(1, 1, 0)[36] as the baseline M0, which is shown to be appropriate for most stations. Indeed, we can achieve better forecasting results by designing station-specific models with different orders. However, as our goal is to evaluate the effect of using the returning flow as a covariate, we still select a universal model for all stations for simplicity.

We use the root mean square error (RMSE) and the symmetric mean absolute percentage error (SMAPE) to evaluate model accuracy:

$$\text{RMSE} = \sqrt{\frac{1}{N} \sum_{t=1}^N (y_t^s - \hat{y}_t^s)^2}, \quad (8)$$

$$\text{SMAPE} = \frac{2}{N} \sum_{t=1}^N \frac{|y_t^s - \hat{y}_t^s|}{|y_t^s| + |\hat{y}_t^s|} \times 100(\%), \quad (9)$$

where  $y_t^s$  and  $\hat{y}_t^s$  are the real boarding flow and the predicted boarding flow, respectively. In addition to RMSE and SMAPE, we also use the Akaike information criterion (AIC) (Akaike, 1998) to measure the trade-off between the goodness of fit and the complexity of a model. A smaller AIC suggests a better model.

### 3.3. Data

We use the passenger flow data retrieved from Guangzhou metro in China as a case study. The smart card data set covers 159 stations from July 24 to September 8 in 2017. Note that the data on weekends are not included in our analysis (i.e., we concatenate Friday with the next Monday), as the RPP has different patterns in weekends. We divide the whole data set into three parts:

- (D1) July 24 to August 4 (two weeks): estimate the RPP  $p_0^s$  for a station  $s$  (for M1 only);
- (D2) August 7 to August 25 (three weeks): estimate model parameters for all the three SARIMA models (training set);
- (D3) August 28 to September 8 (two weeks): evaluate model performance (test set).

After estimating RPP using D1, we compute  $\hat{r}_{t+1}^s$  on data sets D2 and D3 following Eq. (5). Before estimating the SARIMA models, we first empirically examine the relationship between the time series of returning flow  $\hat{r}_t^s$  and the time series of incoming demand  $y_t^s$ . Figure 4 shows the demand time series  $y_t^s$  and the estimated returning flow time series  $\hat{r}_t^s$  on data set D2/D3 for four representative stations. Although the four stations have very diverse demand patterns, we can see that the estimated returning flow  $\hat{r}_t^s$  matches  $y_t^s$  very well. Notably, the returning flow  $\hat{r}_t^s$  makes up a large proportion of the total boarding demand, and it can correctly characterize the temporal dynamics in  $y_t^s$ . More importantly, as marked by the red arrows in panels (a), (c) and (d), the returning flow can even reproduce some irregular increases/drops (i.e., anomalies) of the boarding flow, which are very difficult to capture using conventional time series models with  $y_t^s$  alone.

### 3.4. One-step ahead forecasting

We use data set D2 to estimate model parameters and apply the model to D3 for evaluation. Table 1 shows the results of one-step ahead forecasting for the four stations in Figure 4. Compared with M0, M1 consistently reduces the RMSE and SMAPE of both training and test sets of the four stations by incorporating  $\hat{r}_{t+1}$ . Meanwhile, M1 is also superior with larger log-likelihood and lower AIC. However, with the observed  $r_t^s$  as input, M2 performs almost the same with M0. This might be due to fact that  $r_t^s$  correlates highly with  $y_t^s$  (the observation at the last step), since the returning flow covers a considerable proportion of the overall boarding flow. Thus the amount of additional information brought by this term is rather marginal. While on the contrary,  $\hat{r}_{t+1}^s$  estimated externally by combining RPP and the alighting time series  $m_t^s$  actually encodes the generative mechanisms and long-range dependencies, and thus M1 produces much better forecasting results.

The results in Table 1 indeed show that M1 gives improved accuracy; however, it should be also noted that the improvement varies across different stations. To further explore this variation, we cluster the 159 stations based on their RPPs. In doing so, we transform each RPP into a vector of  $36 \times 36 = 1296$  and perform hierarchical clustering

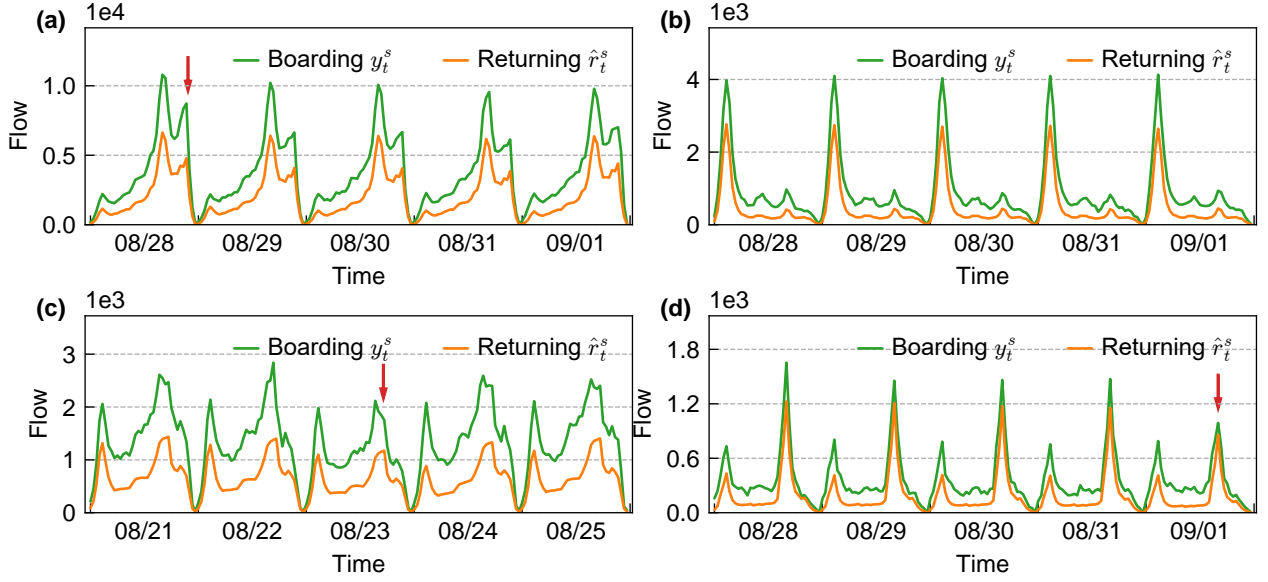


Figure 4: The boarding flow and the estimated returning flow. As marked by red arrows, the returning flow reflects the irregular increases / drops of the boarding flow: (a) Tiyu Xilu station, (b) Luoxi station, (c) Changshou Lu station, and (d) Huijiang station. The green curves represent demand time series  $y_t^s$  and the orange curves correspond to the estimated returning flow time series  $\hat{r}_t^s$ .

Table 1: The one-step boarding flow forecasting of four stations.

Stations	Model	RMSE (train)	RMSE (test)	SMAPE (train)	SMAPE (test)	Log-likelihood	AIC
(a) Tiyu Xilu	M0	398.09	363.06	11.89%	11.63%	-3747.19	7504.37
	M1	<b>372.94</b>	<b>319.60</b>	<b>10.59%</b>	<b>9.29%</b>	<b>-3713.9</b>	<b>7439.79</b>
	M2	396.95	362.00	12.36%	12.22%	-3745.76	7503.52
(b) Luoxi	M0	64.06	71.61	9.51%	9.93%	-2830.25	5670.49
	M1	<b>63.92</b>	<b>71.37</b>	<b>9.48%</b>	<b>9.89%</b>	<b>-2829.25</b>	<b>5670.48</b>
	M2	64.06	71.61	9.51%	9.93%	-2830.25	5672.49
(c) Changshou Lu	M0	93.78	94.34	10.36%	11.88%	-3018.66	6047.31
	M1	<b>90.02</b>	<b>92.74</b>	<b>9.39%</b>	<b>10.83%</b>	<b>-2998.07</b>	<b>6008.15</b>
	M2	93.64	95.16	10.31%	11.99%	-3017.84	6047.67
(d) Huijiang	M0	37.32	47.37	14.05%	14.27%	-2557.94	5125.88
	M1	<b>36.67</b>	<b>38.61</b>	<b>13.49%</b>	<b>13.91%</b>	<b>-2549.47</b>	<b>5110.93</b>
	M2	37.29	47.29	14.05%	14.25%	-2557.61	5127.21

using the Euclidean distance between paired vectors; the distances between clusters are calculated by the Ward’s method (Ward Jr, 1963). In the meanwhile, we measure the effect of  $\hat{r}_{t+1}^s$  by the difference in SMAPE:

$$D^s = \text{SMAPE}_{M1}^s - \text{SMAPE}_{M0}^s, \quad (10)$$

where  $\text{SMAPE}_{M1}^s$  and  $\text{SMAPE}_{M0}^s$  are SMAPE values of M1 and M0, respectively, on the test data set D3. A negative  $D^s$  means M1 improves the forecasting.

The hierarchical clustering in Figure 5 divides the 159 stations into three major clusters. We find that stations cluster 1 mostly corresponds to business-type areas where passengers primarily return in the afternoon or evening, such as in Figure 3 (a). Cluster 2 mainly consists of residential areas that feature a considerable returning flow the next morning, such as in Figure 3 (b). Cluster 3 is a combination of cluster 1 and 2, which has relatively balanced returning flow in both the current and the next day. The bottom panel of Figure 5 shows the  $D^s$  values for all stations following the same order as the clustering result. As can be seen, most stations gives a negative  $D^s$  values, which further confirms the effectiveness of model M1. It should be noted that the effect of  $\hat{r}_{t+1}^s$  are different among clusters. The effect is the most profound for cluster 1 (with two exceptions, which we will discuss in detail in section 3.6), while the least significant for cluster 2. This result suggests that the boarding demand in residential areas can be well



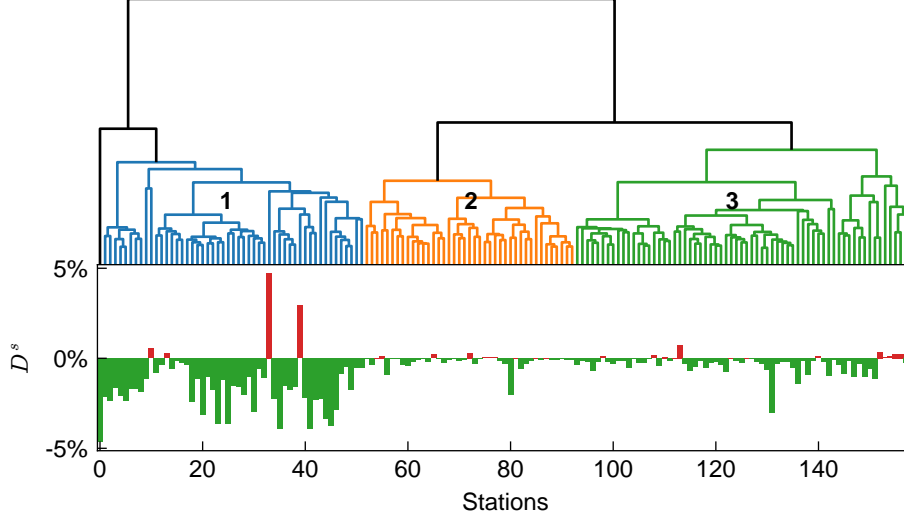


Figure 5: Top: the dendrogram for the hierarchical clustering based on RPP. Bottom: the test set SMAPE differences between M1 and M0; green and negative values means using  $\hat{r}_{t+1}^s$  improves the boarding flow forecast in the test set.

characterized by using only the AR and MA processes.

### 3.5. Multi-step ahead forecasting

Even with strong seasonality, multi-step ahead forecasting is a still challenging task because the errors will accumulate with the rolling forecasting process. A unique advantage of model M1 is that the estimation of returning flow  $\hat{r}_{t+L}^s$  suffers less from this error accumulation problem thanks to the long range dependencies, and even the alighting flow in many steps ago could still dominate the future returning flow. For example, as shown in Figure 3 (a), the alighting flow in the morning (7:00-10:00) plays an important role in determining the returning flow of the evening (17:00-19:00). Therefore, using returning flow as an additional feature in M1 could potentially alleviate the error accumulation problem in multi-step ahead forecasting.

For a  $L$ -step boarding flow forecasting that predicts  $y_{t+L}^s$  by  $y_{1:t}^s$ , M1 requires a series of returning flow  $\hat{r}_{t+1}^s, \dots, \hat{r}_{t+L}^s$  as input. However, in order to estimate  $\hat{r}_{t+L}^s$ , Eq. (5) requires the alighting flow series  $m_{t+1:t+L-1}^s$ , which are not available. In this case, we use the average alighting flow at the same window of historical days as the approximation of future alighting flow  $m_{t+1}^s \dots m_{t+L-1}^s$ . This approximation for the future alighting flow should only bring minor errors to the estimation of returning flow in Eq. (5), since it only contributes to the last  $L - 1$  components in the summation.

We examine the multi-step ahead forecasting using a time series cross-validation method that is known as “evaluation on a rolling forecasting origin” (Hyndman and Athanasopoulos, 2018, Chapter 3). For a  $L$ -step ahead forecasting, we train a model for each observation in data set D3 using a training set form the first observation in data set D2 to the observation  $L$  steps prior to that observation. The error is only evaluated at the  $L^{\text{th}}$  step, and the overall error is the average error over the test set.

Table 2 shows the result of 1, 2, 4, and 6 steps forecasting for M0 and M1. Compared with M0, M1 offers substantially enhanced forecasting in station (a), (c), and (d), and the errors increase much slower with the growing step  $L$ . Especially, in station (a), the RMSE of M0 increases 252.55 (75.6%) form 1-step forecast to 6-step forecast, the number is only 174.66 (60.4%) for M1. For the residential (cluster 2) station (b), the effect of M1 in multi-step ahead forecasting is less significant, which validates the different contributions of returning flow among different clusters. Overall, we can see that multi-step ahead forecasting tasks can benefit substantially from the long-range dependencies encoded in M1 and  $\hat{r}_{t+1}^s$ .

### 3.6. Forecasting under special events

As shown in Figure 5, M1 is less effective only for a few stations. A main reason is that these stations in general have a large variation in RPP from day to day. For these station,  $\hat{r}_{t+1}^s$  will be less accurate and less informative in supporting the forecasting. Therefore, M1 with  $\hat{r}_{t+1}^s$  estimated by a universal RPP will not benefit as much, if not more, than M0 and M2.

Table 2: The multi-step boarding flow forecasting of four stations by time series cross-validation.

Station	Model	30 mins (at $L = 1$ )		1 hour (at $L = 2$ )		2 hours (at $L = 4$ )		3 hours (at $L = 6$ )	
		RMSE	SMAPE	RMSE	SMAPE	RMSE	SMAPE	RMSE	SMAPE
(a) Tiyu Xilu	M0	334.06	12.92%	435.16	15.30%	547.35	19.88%	586.61	19.23%
	M1	<b>290.43</b>	<b>9.87%</b>	<b>328.90</b>	<b>12.60%</b>	<b>403.20</b>	<b>10.82%</b>	<b>465.09</b>	<b>11.71%</b>
(b) Luoxi	M0	<b>75.94</b>	10.64%	79.53	11.70%	88.49	12.14%	90.16	12.51%
	M1	76.10	<b>10.60%</b>	<b>79.43</b>	<b>11.65%</b>	<b>88.49</b>	<b>12.08%</b>	<b>89.97</b>	<b>12.38%</b>
(c) Changshou Lu	M0	97.92	10.28%	126.65	14.42%	154.58	16.74%	168.33	15.89%
	M1	<b>84.80</b>	<b>7.85%</b>	<b>103.84</b>	<b>8.84%</b>	<b>129.53</b>	<b>10.37%</b>	<b>153.12</b>	<b>11.58%</b>
(d) Huijiang	M0	50.27	14.50%	54.09	15.52%	56.16	16.22%	56.30	17.33%
	M1	<b>39.76</b>	<b>13.95%</b>	<b>41.13</b>	<b>14.70%</b>	<b>42.76</b>	<b>15.00%</b>	<b>43.52</b>	<b>15.69%</b>

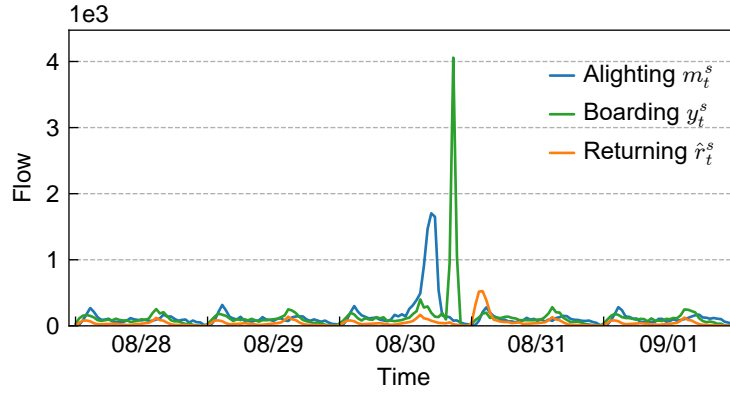


Figure 6: The alighting, boarding, and the estimated returning flow of Luogang station under an event (August 30).

This is particularly the case for forecasting under special events, since the RPP cannot be well estimated using historical data and it will involve large variation in nature. For example, as a metro station next to the Guangzhou International Sports Arena, Luogang often experiences surging demand because of large sports events and concerts. Figure 6 shows that the come-and-return dynamics under the special event is very different from normal days. The event in August 30 brought a period of unusually high alighting flow. After the event, the returning passengers caused another peak in the boarding flow. If we adopt a universal RPP estimated by aggregating historical data, we will end up with erroneously distributing the returning flow to the next morning (the morning peak of  $\hat{r}_t^s$  on August 31). To address this problem, we propose to build two separate RPPs for normal and event-induced passengers, respectively. For the passengers alight at time  $t_a$ , the probability of returning at  $t$  becomes the weighted sum of the two parts:

$$p^s(\tau_{\text{boarding}} = t \mid \tau_{\text{alighting}} = t_a) = \frac{m_{t_a}^{s,e}}{m_{t_a}^s} p^{s,e}(\tau_{\text{boarding}} = t \mid \tau_{\text{alighting}} = t_a) + \frac{m_{t_a}^{s,n}}{m_{t_a}^s} p^{s,n}(\tau_{\text{boarding}} = t \mid \tau_{\text{alighting}} = t_a), \quad (11)$$

where we use superscript  $e$  and  $n$  to denote variables for event and normal condition, and the alighting flow  $m_{t_a}^s = m_{t_a}^{s,e} + m_{t_a}^{s,n}$ . When the event-induced alighting flow  $m_{t_a}^{s,e} = 0$ , Eq. (11) reduces to the normal RPP.

In practice, we have a few approaches to estimate the event-induced alighting flow  $m_{t_a}^{s,e}$  and RPP under events, such as looking into the passenger flow of the specific gate to the event venue or using the time information of an event. When such information is not available, we propose to apply the following method to estimate the RPP under events (assuming all events in station  $s$  follow the same RPP). First, a period with alighting flow larger than a threshold is identified as an event period. For each time window in a day, we use  $Q_3 + 1.5(IQR)$  as the threshold, where  $Q_3$  is the third quartile and  $IQR$  the interquartile range. Next, the normal RPP can be estimated by the non-event periods. Subtracting the normal alighting (use median) and the normal returning flow from the part identified as event periods, the rest data in event periods are used to estimate the RPP under special events. By separating event and normal flow, we also prevent the normal RPP from being influenced by the event flow.

Using the data from from July 1 to August 24, 2017 (weekends included), Figure 7 shows the event RPP of

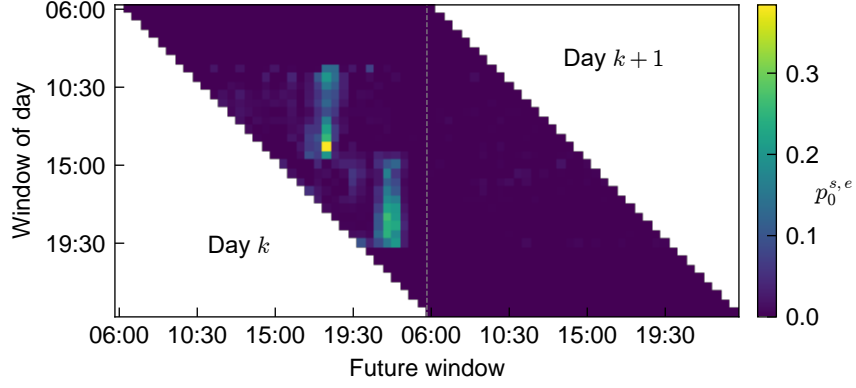


Figure 7: The RPP for passenger flow induced by events in Luogang station. Probabilities are set to zero for time windows without event.

Luogang station. It is conspicuous that two types of events exist in this venue, one ends in the afternoon and the other ends in the evening. The returning time for each type of event is more concentrated than the alighting time and is mostly on the same day of the alighting time. Although the RPP is estimated from different events (8 days with significant events), the return probability of these events shows regular and predictive patterns.

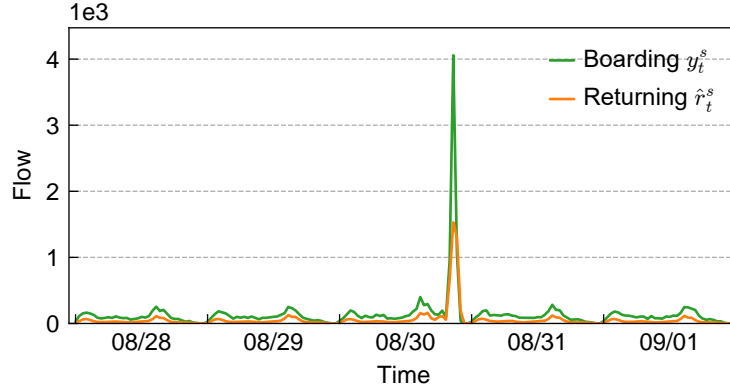


Figure 8: The boarding and the returning flow (using Eq. (11)) of Luogang station.

Figure 8 shows the re-estimated returning flow of Luogang station. Compared with Figure 6, we can find the returning flow in Figure 8 can now correctly reflect the peak and trend of the boarding flow under the special event. Note that the days in Figure 8 are different the days used for event RPP estimation, which shows the come-and-return dynamic of different events in this station follows similar patterns.

Considering that these events are occasional, we use the non-seasonal ARIMA with the order  $\text{ARIMA}(2, 0, 1)$  as our baseline model M0. The data separation is the same as section 3.3 except that we use a longer period for the event RPP estimation. We denote by M1' the ARIMA-X model that uses the “adjusted” returning flow as a covariate. The forecasting results are shown in Table 3. M1' gives the best performance in RMSE, Log-likelihood, and AIC, while M1 is the best in terms of SMAPE. Due to the considerable difference in the magnitude of boarding flow under event and normal condition and many near-zero volumes in off-peak time, the best model suggested by RMSE and SMAPE is different. The results further shows that the returning flow offers substantial improvement even for the forecasting under special events. Although the simple ARIMA may not be the best model for a time series with apparent “outliers” such as these events, the returning flow could be easily integrated into other models for better prediction.

#### 4. Conclusions and discussion

In this paper, we propose a new framework for forecasting passenger flow time series in metro systems. Different from previous studies that capture temporal dynamics in a data-driven way, we incorporate the generative

Table 3: The boarding flow forecasting of Luogang stations.

Model	RMSE (train)	RMSE (test)	SMAPE (train)	SMAPE (test)	Log-likelihood	AIC
M0	61.35	218.27	52.74%	56.07%	-2984.11	5978.22
M1	53.40	228.29	<b>40.67%</b>	<b>46.04%</b>	-2909.38	5830.76
M1'	<b>45.37</b>	<b>153.89</b>	46.12%	49.44%	<b>-2821.29</b>	<b>5654.58</b>
M2	60.06	207.16	50.35%	51.28%	-2972.46	5956.92

mechanisms rooted in travel behavior into the modeling of passenger flow time series. In doing so, we introduce returning flow as a new covariate/feature into standard time series models. The returning flow is estimated as the expected returning boarding demand given previous alighting trips; thus, it encodes the causal structure and long-range dependencies in passenger flow data. We estimate the return probability by aggregating historical data, which also avoids the sensitivity issues and privacy concerns of using individual-based data/models such as in Zhao et al. (2018). We examine this new framework on a real-world passenger flow data set collected from Guangzhou metro in China, and the proposed framework with returning flow has demonstrated superior performance in various scenarios, including one-step ahead forecasting, multi-step ahead forecasting, and forecasting under special events.

There are several directions to explore for future research. First, we assume that both the boarding and the alighting time series are available (i.e., both tapping-in and tapping-out are registered by the smart card system), while metro in some cities may have a tapping-in only smart card system. In this case, one can further integrate a destination inference model (see e.g., Barry et al., 2002; Trépanier et al., 2007) into the proposed framework. Second, we use a simple and standard SARIMA model to assess the effectiveness of the proposed framework; in practice, we think the forecasting performance can be further improved by using more advanced statistical time series and deep learning-based sequence models. Third, current framework is station-specific, while the travel behavior regularity is ubiquitous and different stations may exhibit similar patterns. Thus, an interesting direction is to develop new models to generalize the causal structure across different stations, such as applying matrix/tensor factorization method (Sun and Axhausen, 2016) to learn the structure of RPP. Fourth, the returning flow in the current form must have the same boarding station as the previous alighting station; in fact, we can relax this assumption and build a network-wide model based on the causal structure among trips. Finally, this framework can be extended to other transport modes with non-random and chained travel patterns, such as private vehicles, taxi, and ride-hailing service. This paper also sheds new light on other behavior-driven demand forecasting problems, in which the causal structure and the long-range dependencies play a substantial role. For example, integrating purchasing behavior into the demand forecasting of retail products.

## Acknowledgement

This research is supported by the Natural Sciences and Engineering Research Council (NSERC) of Canada, Mitacs, exo.quebec (<https://exo.quebec/en>), the Institute for Data Valorisation (IVADO), and the Canada Foundation for Innovation (CFI).

## References

- Akaike, H., 1998. Information theory and an extension of the maximum likelihood principle, in: Selected papers of hirotugu akaike. Springer, pp. 199–213.
- Barry, J.J., Newhouser, R., Rahbee, A., Sayeda, S., 2002. Origin and destination estimation in new york city with automated fare system data. *Transportation Research Record* 1817, 183–187.
- Chen, E., Ye, Z., Wang, C., Xu, M., 2020a. Subway passenger flow prediction for special events using smart card data. *IEEE Transactions on Intelligent Transportation Systems* 21, 1109–1120.
- Chen, J., Liu, L., Wu, H., Zhen, J., Li, G., Lin, L., 2020b. Physical-virtual collaboration graph network for station-level metro ridership prediction. *arXiv preprint arXiv:2001.04889*.
- Chen, Q., Li, W., Zhao, J., 2011. The use of ls-svm for short-term passenger flow prediction. *Transport* 26, 5–10.
- Dickey, D.A., Fuller, W.A., 1979. Distribution of the estimators for autoregressive time series with a unit root. *Journal of the American Statistical Association* 74, 427–431.

- Ding, C., Duan, J., Zhang, Y., Wu, X., Yu, G., 2017. Using an ARIMA-GARCH modeling approach to improve subway short-term ridership forecasting accounting for dynamic volatility. *IEEE Transactions on Intelligent Transportation Systems* 19, 1054–1064.
- Gong, Y., Li, Z., Zhang, J., Liu, W., Zheng, Y., Kirsch, C., 2018. Network-wide crowd flow prediction of sydney trains via customized online non-negative matrix factorization, in: *Proceedings of the 27th ACM International Conference on Information and Knowledge Management*, pp. 1243–1252.
- Goulet-Langlois, G., Koutsopoulos, H.N., Zhao, Z., Zhao, J., 2017. Measuring regularity of individual travel patterns. *IEEE Transactions on Intelligent Transportation Systems* 19, 1583–1592.
- Hao, S., Lee, D.H., Zhao, D., 2019. Sequence to sequence learning with attention mechanism for short-term passenger flow prediction in large-scale metro system. *Transportation Research Part C: Emerging Technologies* 107, 287–300.
- Hyndman, R.J., Athanasopoulos, G., 2018. *Forecasting: principles and practice*. 2nd ed., OTexts, Melbourne, Australia.
- Jiao, P., Li, R., Sun, T., Hou, Z., Ibrahim, A., 2016. Three revised kalman filtering models for short-term rail transit passenger flow prediction. *Mathematical Problems in Engineering* 2016, 9717582.
- Li, Y., Wang, X., Sun, S., Ma, X., Lu, G., 2017. Forecasting short-term subway passenger flow under special events scenarios using multiscale radial basis function networks. *Transportation Research Part C: Emerging Technologies* 77, 306–328.
- Liu, Y., Liu, Z., Jia, R., 2019. Deeppf: A deep learning based architecture for metro passenger flow prediction. *Transportation Research Part C: Emerging Technologies* 101, 18–34.
- Stathopoulos, A., Karlaftis, M.G., 2003. A multivariate state space approach for urban traffic flow modeling and prediction. *Transportation Research Part C: Emerging Technologies* 11, 121–135.
- Sun, L., Axhausen, K.W., 2016. Understanding urban mobility patterns with a probabilistic tensor factorization framework. *Transportation Research Part B: Methodological* 91, 511–524.
- Sun, L., Axhausen, K.W., Lee, D.H., Huang, X., 2013. Understanding metropolitan patterns of daily encounters. *Proceedings of the National Academy of Sciences* 110, 13774–13779.
- Sun, Y., Leng, B., Guan, W., 2015. A novel wavelet-svm short-time passenger flow prediction in beijing subway system. *Neurocomputing* 166, 109–121.
- Tan, M.C., Wong, S.C., Xu, J.M., Guan, Z.R., Zhang, P., 2009. An aggregation approach to short-term traffic flow prediction. *IEEE Transactions on Intelligent Transportation Systems* 10, 60–69.
- Toqué, F., Khouadja, M., Come, E., Trepanier, M., Oukhellou, L., 2017. Short & long term forecasting of multimodal transport passenger flows with machine learning methods, in: *IEEE 20th International Conference on Intelligent Transportation Systems (ITSC)*, pp. 560–566.
- Trépanier, M., Tranchant, N., Chapleau, R., 2007. Individual trip destination estimation in a transit smart card automated fare collection system. *Journal of Intelligent Transportation Systems* 11, 1–14.
- Tsai, T.H., Lee, C.K., Wei, C.H., 2009. Neural network based temporal feature models for short-term railway passenger demand forecasting. *Expert Systems with Applications* 36, 3728–3736.
- Union Internationale des Transports Publics (UITP), 2018. World metro figure 2018 statistic brief. <https://www.uitp.org/world-metro-figures-2018>. Accessed: 2020-03-20.
- Vlahogianni, E.I., Karlaftis, M.G., Golias, J.C., 2005. Optimized and meta-optimized neural networks for short-term traffic flow prediction: A genetic approach. *Transportation Research Part C: Emerging Technologies* 13, 211–234.
- Ward Jr, J.H., 1963. Hierarchical grouping to optimize an objective function. *Journal of the American statistical association* 58, 236–244.
- Williams, B.M., Hoel, L.A., 2003. Modeling and forecasting vehicular traffic flow as a seasonal ARIMA process: Theoretical basis and empirical results. *Journal of Transportation Engineering* 129, 664–672.
- Zhao, Z., Koutsopoulos, H.N., Zhao, J., 2018. Individual mobility prediction using transit smart card data. *Transportation Research Part C: Emerging Technologies* 89, 19–34.